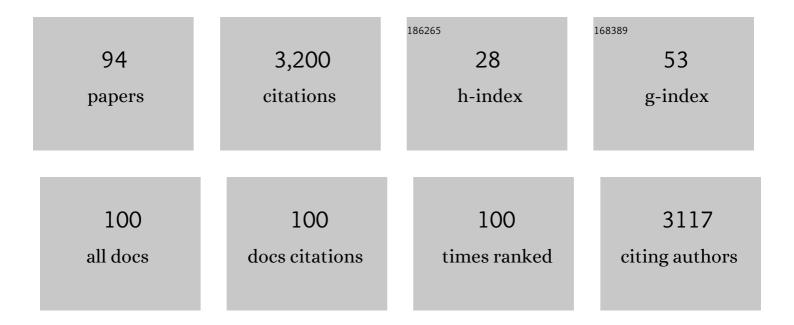
## Daniel Wüstner

List of Publications by Year in descending order

Source: https://exaly.com/author-pdf/9572966/publications.pdf Version: 2024-02-01



#	Article	IF	CITATIONS
1	Vesicular and Non-vesicular Sterol Transport in Living Cells. Journal of Biological Chemistry, 2002, 277, 609-617.	3.4	269
2	Intracellular cholesterol transport. Journal of Clinical Investigation, 2002, 110, 891-898.	8.2	254
3	Analysis of Cholesterol Trafficking with Fluorescent Probes. Methods in Cell Biology, 2012, 108, 367-393.	1.1	203
4	Intracellular cholesterol transport. Journal of Clinical Investigation, 2002, 110, 891-898.	8.2	136
5	Fluorescent sterols as tools in membrane biophysics and cell biology. Chemistry and Physics of Lipids, 2007, 146, 1-25.	3.2	135
6	Structural Insight into Eukaryotic Sterol Transport through Niemann-Pick Type C Proteins. Cell, 2019, 179, 485-497.e18.	28.9	110
7	Rapid Nonvesicular Transport of Sterol between the Plasma Membrane Domains of Polarized Hepatic Cells. Journal of Biological Chemistry, 2002, 277, 30325-30336.	3.4	101
8	Direct Observation of Rapid Internalization and Intracellular Transport of Sterol by Macrophage Foam Cells. Traffic, 2005, 6, 396-412.	2.7	88
9	Rapid Transbilayer Movement of the Fluorescent Sterol Dehydroergosterol in Lipid Membranes. Biophysical Journal, 2002, 83, 1525-1534.	0.5	87
10	Rapid Flip-Flop of Phospholipids in Endoplasmic Reticulum Membranes Studied by a Stopped-Flow Approach. Biophysical Journal, 2000, 78, 2628-2640.	0.5	85
11	Variable domain-linked oligosaccharides of a human monoclonal IgG: structure and influence on antigen binding. Biochemical Journal, 1999, 338, 529-538.	3.7	84
12	A comparative study on fluorescent cholesterol analogs as versatile cellular reporters. Journal of Lipid Research, 2016, 57, 299-309.	4.2	78
13	Different transport routes for high density lipoprotein and its associated free sterol in polarized hepatic cells. Journal of Lipid Research, 2004, 45, 427-437.	4.2	72
14	Plasma Membrane Sterol Distribution Resembles the Surface Topography of Living Cells. Molecular Biology of the Cell, 2007, 18, 211-228.	2.1	66
15	Ergosterol is mainly located in the cytoplasmic leaflet of the yeast plasma membrane. Traffic, 2018, 19, 198-214.	2.7	62
16	How cholesterol interacts with proteins and lipids during its intracellular transport. Biochimica Et Biophysica Acta - Biomembranes, 2015, 1848, 1908-1926.	2.6	61
17	Membrane Orientation and Lateral Diffusion of BODIPY-Cholesterol as a Function of Probe Structure. Biophysical Journal, 2013, 105, 2082-2092.	0.5	60
18	Quantitative assessment of sterol traffic in living cells by dual labeling with dehydroergosterol and BODIPY-cholesterol. Chemistry and Physics of Lipids, 2011, 164, 221-235.	3.2	57

#	Article	IF	CITATIONS
19	The role of ABC proteins Aus1p and Pdr11p in the uptake of external sterols in yeast: Dehydroergosterol fluorescence study. Biochemical and Biophysical Research Communications, 2011, 404, 233-238.	2.1	46
20	Quantitative fluorescence loss in photobleaching for analysis of protein transport and aggregation. BMC Bioinformatics, 2012, 13, 296.	2.6	46
21	Kinetic imaging of NPC1L1 and sterol trafficking between plasma membrane and recycling endosomes in hepatoma cells. Journal of Lipid Research, 2008, 49, 2023-2037.	4.2	42
22	Selective Visualization of Fluorescent Sterols in Caenorhabditis elegans by Bleach-Rate-Based Image Segmentation. Traffic, 2010, 11, 440-454.	2.7	39
23	Photobleaching Kinetics and Time-Integrated Emission of Fluorescent Probes in Cellular Membranes. Molecules, 2014, 19, 11096-11130.	3.8	39
24	Vesicular and Nonvesicular Transport of Phosphatidylcholine in Polarized HepG2 Cells. Traffic, 2001, 2, 277-296.	2.7	38
25	The fluorescent cholesterol analog dehydroergosterol induces liquid-ordered domains in model membranes. Chemistry and Physics of Lipids, 2009, 159, 114-118.	3.2	37
26	Mathematical Analysis of Hepatic High Density Lipoprotein Transport Based on Quantitative Imaging Data. Journal of Biological Chemistry, 2005, 280, 6766-6779.	3.4	34
27	Potential of BODIPY-cholesterol for analysis of cholesterol transport and diffusion in living cells. Chemistry and Physics of Lipids, 2016, 194, 12-28.	3.2	32
28	<scp>SpatTrack</scp> : An Imaging Toolbox for Analysis of Vesicle Motility and Distribution in Living Cells. Traffic, 2014, 15, 1406-1429.	2.7	31
29	Dehydroergosterol as an Analogue for Cholesterol: Why It Mimics Cholesterol So Well—or Does It?. Journal of Physical Chemistry B, 2014, 118, 7345-7357.	2.6	31
30	Rapid Nonvesicular Transport of Sterol between the Plasma Membrane Domains of Polarized Hepatic Cells. Journal of Biological Chemistry, 2002, 277, 30325-30336.	3.4	29
31	Improved visualization and quantitative analysis of fluorescent membrane sterol in polarized hepatic cells. Journal of Microscopy, 2005, 220, 47-64.	1.8	27
32	Using internal and collective variables in Monte Carlo simulations of nucleic acid structures: Chain breakage/closure algorithm and associated Jacobians. Journal of Computational Chemistry, 2006, 27, 309-315.	3.3	27
33	Live Cell Linear Dichroism Imaging Reveals Extensive Membrane Ruffling within the Docking Structure of Natural Killer Cell Immune Synapses. Biophysical Journal, 2009, 96, L13-L15.	0.5	27
34	Potential of ultraviolet wideâ€field imaging and multiphoton microscopy for analysis of dehydroergosterol in cellular membranes. Microscopy Research and Technique, 2011, 74, 92-108.	2.2	26
35	Fluorescent Sterols and Cholesteryl Esters as Probes for Intracellular Cholesterol Transport. Lipid Insights, 2015, 8s1, LPI.S31617.	1.0	26
36	Head group-independent interaction of phospholipids with bile salts: a fluorescence and EPR study. Journal of Lipid Research, 2000, 41, 395-404.	4.2	23

#	Article	IF	CITATIONS
37	Spatiotemporal analysis of endocytosis and membrane distribution of fluorescent sterols in living cells. Histochemistry and Cell Biology, 2008, 130, 891-908.	1.7	22
38	Imaging approaches for analysis of cholesterol distribution and dynamics in the plasma membrane. Chemistry and Physics of Lipids, 2016, 199, 106-135.	3.2	22
39	Niemann Pick C2 protein enables cholesterol transfer from endo-lysosomes to the plasma membrane for efflux by shedding of extracellular vesicles. Chemistry and Physics of Lipids, 2021, 235, 105047.	3.2	21
40	Chromatic aberration correction and deconvolution for UV sensitive imaging of fluorescent sterols in cytoplasmic lipid droplets. Cytometry Part A: the Journal of the International Society for Analytical Cytology, 2008, 73A, 727-744.	1.5	20
41	Glycosylation analysis of a polyreactive human monoclonal IgG antibody derived from a human-mouse heterohybridoma. Molecular Immunology, 1995, 32, 595-602.	2.2	19
42	Embedding beyond electrostatics—The role of wave function confinement. Journal of Chemical Physics, 2016, 145, 104102.	3.0	19
43	Niemann-Pick C2 protein regulates sterol transport between plasma membrane and late endosomes in human fibroblasts. Chemistry and Physics of Lipids, 2018, 213, 48-61.	3.2	19
44	Bayesian model selection with fractional Brownian motion. Journal of Statistical Mechanics: Theory and Experiment, 2018, 2018, 093501.	2.3	19
45	Quantitative imaging of membrane contact sites for sterol transfer between endo-lysosomes and mitochondria in living cells. Scientific Reports, 2021, 11, 8927.	3.3	19
46	Substituted 9-Diethylaminobenzo[ <i>a</i> ]phenoxazin-5-ones (Nile Red Analogues): Synthesis and Photophysical Properties. Journal of Organic Chemistry, 2021, 86, 1471-1488.	3.2	19
47	Pathways and Mechanisms of Cellular Cholesterol Efflux—Insight From Imaging. Frontiers in Cell and Developmental Biology, 2022, 10, 834408.	3.7	19
48	Variable domain-linked oligosaccharides of a human monoclonal IgG: structure and influence on antigen binding. Biochemical Journal, 1999, 338 ( Pt 2), 529-38.	3.7	18
49	Design of new fluorescent cholesterol and ergosterol analogs: Insights from theory. Biochimica Et Biophysica Acta - Biomembranes, 2015, 1848, 2188-2199.	2.6	17
50	Computational Analysis of Sterol Ligand Specificity of the Niemann Pick C2 Protein. Biochemistry, 2016, 55, 5165-5179.	2.5	17
51	Variable domain-linked oligosaccharides of a human monoclonal IgG: structure and influence on antigen binding. Biochemical Journal, 1999, 338, 529.	3.7	16
52	Aminophospholipids Have No Access to the Luminal Side of the Biliary Canaliculus. Journal of Biological Chemistry, 2003, 278, 40631-40639.	3.4	16
53	Two-photon time-lapse microscopy of BODIPY-cholesterol reveals anomalous sterol diffusion in chinese hamster ovary cells. BMC Biophysics, 2012, 5, 20.	4.4	16
54	A comparison of single particle tracking and temporal image correlation spectroscopy for quantitative analysis of endosome motility. Journal of Microscopy, 2013, 252, 169-188.	1.8	15

#	Article	IF	CITATIONS
55	One- and two-photon solvatochromism of the fluorescent dye Nile Red and its CF3, F and Br-substituted analogues. Photochemical and Photobiological Sciences, 2020, 19, 1382-1391.	2.9	15
56	Head group-independent interaction of phospholipids with bile salts. A fluorescence and EPR study. Journal of Lipid Research, 2000, 41, 395-404.	4.2	15
57	Release of Phospholipids from Erythrocyte Membranes by Taurocholate Is Determined by Their Transbilayer Orientation and Hydrophobic Backbone. Biochemistry, 1998, 37, 17093-17103.	2.5	14
58	Free-cholesterol loading does not trigger phase separation of the fluorescent sterol dehydroergosterol in the plasma membrane of macrophages. Chemistry and Physics of Lipids, 2008, 154, 129-136.	3.2	14
59	Synthesis and Live-Cell Imaging of Fluorescent Sterols for Analysis of Intracellular Cholesterol Transport. Methods in Molecular Biology, 2017, 1583, 111-140.	0.9	14
60	Following Intracellular Cholesterol Transport by Linear and Non-Linear Optical Microscopy of Intrinsically Fluorescent Sterols. Current Pharmaceutical Biotechnology, 2012, 13, 303-318.	1.6	13
61	Cholesterol binding to the sterol-sensing region of Niemann Pick C1 protein confines dynamics of its N-terminal domain. PLoS Computational Biology, 2020, 16, e1007554.	3.2	12
62	Structural design of intrinsically fluorescent oxysterols. Chemistry and Physics of Lipids, 2018, 212, 26-34.	3.2	11
63	Binding and intracellular transport of 25-hydroxycholesterol by Niemann-Pick C2 protein. Biochimica Et Biophysica Acta - Biomembranes, 2020, 1862, 183063.	2.6	11
64	Quantification of polarized trafficking of transferrin and comparison with bulk membrane transport in hepatic cells. Biochemical Journal, 2006, 400, 267-280.	3.7	10
65	Transient accumulation and bidirectional movement of KIF13B in primary cilia. Journal of Cell Science, 2023, 136, .	2.0	10
66	The Second-Order Polarization Propagator Approximation (SOPPA) method coupled to the polarizable continuum model. Computational and Theoretical Chemistry, 2014, 1040-1041, 54-60.	2.5	9
67	Mechanistic Insight into Lipid Binding to Yeast Niemann Pick Type C2 Protein. Biochemistry, 2020, 59, 4407-4420.	2.5	9
68	Steady State Analysis and Experimental Validation of a Model for Hepatic High-Density Lipoprotein Transport. Traffic, 2006, 7, 699-715.	2.7	8
69	Membrane organization and intracellular transport of a fluorescent analogue of 27-hydroxycholesterol. Chemistry and Physics of Lipids, 2020, 233, 105004.	3.2	8
70	Direct observation of nystatin binding to the plasma membrane of living cells. Biochimica Et Biophysica Acta - Biomembranes, 2021, 1863, 183528.	2.6	8
71	Multicolor bleach-rate imaging enlightens in vivo sterol transport. Communicative and Integrative Biology, 2010, 3, 370-373.	1.4	7
72	Liveâ€cell imaging of new polyene sterols for improved analysis of intracellular cholesterol transport. Journal of Microscopy, 2018, 271, 36-48.	1.8	7

#	Article	IF	CITATIONS
73	Atomistic Monte Carlo Simulation of Lipid Membranes. International Journal of Molecular Sciences, 2014, 15, 1767-1803.	4.1	6
74	Rational design of novel fluorescent analogues of cholesterol: a "step-by-step―computational study. Physical Chemistry Chemical Physics, 2019, 21, 15487-15503.	2.8	6
75	Computational Modeling Explains the Multi Sterol Ligand Specificity of the N-Terminal Domain of Niemann–Pick C1-Like 1 Protein. ACS Omega, 2019, 4, 20894-20904.	3.5	6
76	Intracellular Cholesterol Transport. , 2009, , 157-190.		6
77	Computational Characterization of a Cholesterol-Based Molecular Rotor in Lipid Membranes. Journal of Physical Chemistry B, 2019, 123, 7313-7326.	2.6	5
78	Dynamic Mode Decomposition of Fluorescence Loss in Photobleaching Microscopy Data for Model-Free Analysis of Protein Transport and Aggregation in Living Cells. Sensors, 2022, 22, 4731.	3.8	5
79	Computational modeling of fluorescence loss in photobleaching. Computing and Visualization in Science, 2015, 17, 151-166.	1.2	4
80	A Discontinuous Galerkin Model for Fluorescence Loss in Photobleaching. Scientific Reports, 2018, 8, 1387.	3.3	4
81	Modeling the Sterol-Binding Domain of Aster-A Provides Insight into Its Multiligand Specificity. Journal of Chemical Information and Modeling, 2020, 60, 2268-2281.	5.4	4
82	Photophysical and Structural Characterization of Intrinsically Fluorescent Sterol Aggregates. Journal of Physical Chemistry B, 2021, 125, 5838-5852.	2.6	4
83	Steady state analysis of influx and transbilayer distribution of ergosterol in the yeast plasma membrane. Theoretical Biology and Medical Modelling, 2019, 16, 13.	2.1	3
84	Quantitative Fluorescence Studies of Intracellular Sterol Transport and Distribution. Springer Series on Fluorescence, 2012, , 185-213.	0.8	2
85	Photophysical investigation of two emissive nucleosides exhibiting gigantic stokes shifts. Photochemical and Photobiological Sciences, 2019, 18, 1858-1865.	2.9	2
86	Design, Synthesis, and Evaluation of a Luminescent Cholesterol Mimic. Journal of Organic Chemistry, 2021, 86, 1612-1621.	3.2	2
87	Quantitative Co-Localization and Pattern Analysis of Endo-Lysosomal Cargo in Subcellular Image Cytometry and Validation on Synthetic Image Sets. Methods in Molecular Biology, 2017, 1594, 93-128.	0.9	1
88	A discontinuous Galerkin model for fluorescence loss in photobleaching of intracellular polyglutamine protein aggregates. BMC Biophysics, 2018, 11, 7.	4.4	1
89	Mechanism of Cholesterol Sensing in the Niemann Pick Protein (NPC1) using Molecular Dynamics Simulations. Biophysical Journal, 2019, 116, 300a.	0.5	0
90	Computational analysis of altered one- and two-photon CD of sterols inside a protein binding pocket. Theoretical Chemistry Accounts, 2022, 141, 1.	1.4	0

#	Article	IF	CITATIONS
91	Title is missing!. , 2020, 16, e1007554.		Ο
92	Title is missing!. , 2020, 16, e1007554.		0
93	Title is missing!. , 2020, 16, e1007554.		0
94	Title is missing!. , 2020, 16, e1007554.		0